Supplementary Information

Ultrafast photothermal shock for crystallization of vanadium oxide and in situ anchoring of Co single atoms for enhanced oxygen evolution reaction

Dogyeong Jeon [a], Heejun Park [a], Jong Won Baek [a], Ki Ro Yoon [b], Sang-Joon Kim [*c], and Il-Doo Kim [*a]

[a]Department of Materials Science and Engineering, Korea Advanced Institute of Science and Technology (KAIST), 291 Daehak-ro, Yuseong-gu, Daejeon 34141, Republic of Korea

[b]Department of Materials Science and Engineering, Konkuk University, 120, Neungdong-ro, Gwangjin-gu, Seoul 05029, Republic of Korea

[c]Department of Materials Science and Engineering, Chungnam National University (CNU), 99 Daehak-ro, Yuseong-gu, Daejeon 34134, Republic of Korea.

* E-mail: sangjoon@cnu.ac.kr, idkim@kaist.ac.kr

Table of Contents

Supplementary Experimental Procedures

Preparation of Co@VO_x@CNF

The preparation of the Co/VO_x/CNF electrode began with the fabrication of the carbon nanofiber (CNF) scaffold, where electrospun polyacrylonitrile (PAN) nanofibers were stabilized at 250 °C for 2 h in air and subsequently carbonized at 1,500 °C for 2 h under an Ar atomosphere. After an O_2 plasma treatment to improve hydrophilicity, an amorphous vanadium oxide (VO_x) layer was conformally coated onto the CNF via electrodeposition for an optimized duration of 10 minutes. For the single-atom functionalization, a 0.1 M cobalt (II) chloride hexahydrate solution prepared in DI water was drop-cast onto the as-prepared amorphous VO_x/CNF electrode and fully dried. The precursor-loaded electrode was then subjected to an ultrafast photothermal shock using an intense pulsed light (IPL) system (PLT, South Korea) equipped with a Xenon flash lamp (broad spectrum: 300–1000 nm). The photothermal process was conducted under ambient conditions with a lamp-to-sample distance of 2 cm, a constant input voltage of 200 V–500 V, and a pulse duration of 20 ms. By controlling the energy density at 8 J cm^{-2} and 10 J cm^{-2}, the temperature was instantaneously elevated to approximately 700 °C (Co/VO_x/CNF-L) and 1,600 °C (Co/VO_x/CNF-H), respectively.

Characterization

The microstructure was studied in detail with a field-emission scanning electron microscope (SEM; Hitachi SU8230, Hitachi, Tokyo, Japan). XRD measurements (D/MAX-2500, Rigaku) were performed using a high-resolution powder X-ray diffractometer with Cu Kα radiation. XPS (Sigma Probe, Thermo VG Scientific) was carried out using Al Kα radiation. Transmission electron microscopy (TEM), the high-angle annular dark-field scanning TEM (HADDF-STEM) and energy dispersive X-ray spectroscopy (EDS) analysis were carried out by double-aberration-corrected TEM (Titan Themis-3 Double Cs & Mono, FEI; Titan cubed G2 60–300) equipped with Chemi-STEM and X-FEG system. XAS measurements were performed on beamline 8C at the Pohang Accelerator Laboratory (PAL, Pohang, South Korea). All XAS spectra were acquired at room temperature in fluorescence mode using a double-crystal Si (111) monochromator. Analyses of both the near edge (in energy scale) and extended range (in R space) XAS spectra were performed using Larix software, and fitting was

performed using JAI-EXAFS. The use of JAI-EXAFS followed the procedure reported by Jeong et al. (Sci. Rep. 15, 17417, 2025).

Electrochemical Measurement

Electrochemical measurements were performed in a three-electrode electrochemical setup using a Wonatech Zive MP1 multichannel potentiostat. The as-prepared self-supported $Co/VO_x/CNF$ electrode was directly used as the working electrode, while a Pt wire and a Ag/AgCl (saturated KCl) electrode served as the counter and reference electrodes, respectively. All measured potentials were converted to the reversible hydrogen electrode (RHE) scale according to the Nernst equation ($E_{RHE} = E_{Ag/AgCl} + 0.197\ V + 0.059 \times pH$), and the polarization curves were corrected for ohmic losses (iR-correction) to reflect intrinsic catalytic activity. Prior to recording the data, the working electrode was activated via cyclic voltammetry (CV) scans until stable curves were obtained. The OER activity was evaluated using linear sweep voltammetry (LSV). To assess the accelerated durability, the catalyst was subjected to 300 continuous CV cycles within the potential range of 1.3–1.6 V vs. RHE, after which the polarization curve remained nearly identical to the initial state. Furthermore, long-term stability was examined via chronopotentiometry (CP), demonstrating a stable potential retention at a constant current density of 10 mA cm^{-2} for over 35 hours.

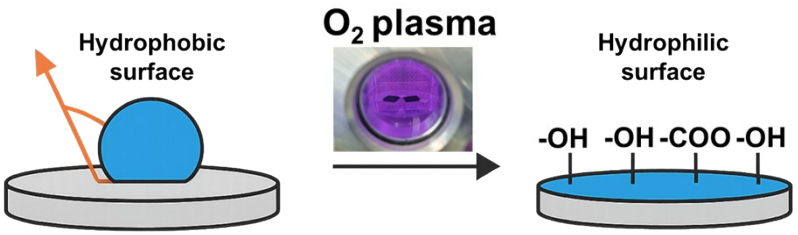

Figure S1. Schematic of O_2 plasma surface activation of a CNF support.

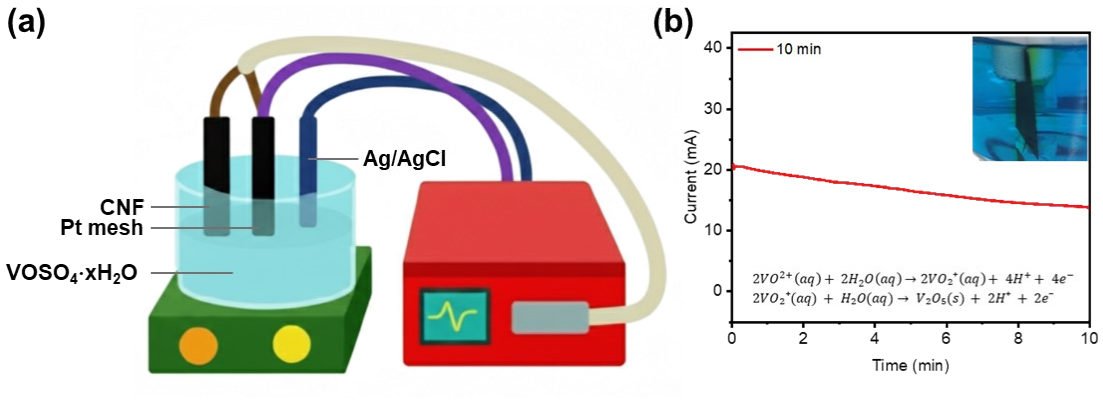

Figure S2. Electrodeposition on a CNF working electrode. (a) A three-electrode setup (CNF working, Pt mesh counter, Ag/AgCl reference) under potentiostatic control. (b) Chronoamperometric current–time curve. Under acidic vanadyl-sulfate conditions (pH =1.8, 65 °C), applying 1.2 V drives a two-stage process on the hydrophilic, porous CNF. First, VO^{2+} species are enriched at the CNF/electrolyte interface by diffusion and undergo anodic conversion to VO_2^+, establishing a VO_2^+-rich interphase. Next, continued interfacial oxidation coupled with hydrolysis nucleates and grows V_2O_5, yielding a conformal, adherent VO_x (V_2O_5-dominant) coating across the CNF scaffold. After a 10-min deposition, the immersed CNF (inset) displays a uniform VO_x layer with strong adhesion to the fibrous scaffold.

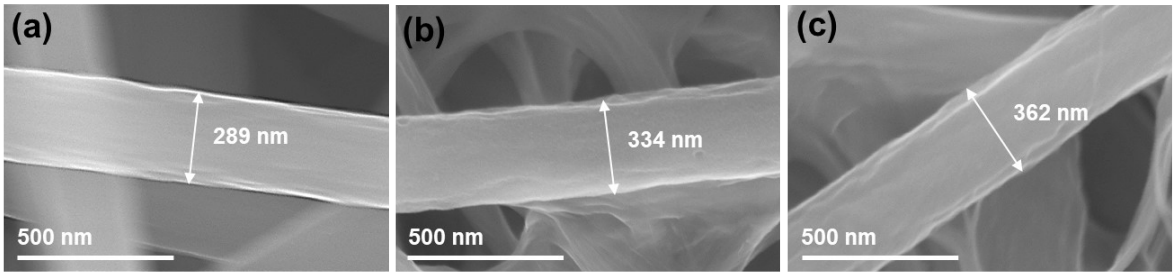

Figure S3. SEM images of VO_x-electrodeposited CNF at varying deposition times. (a) 0 min, (b) 10 min, and (c) 30 min.

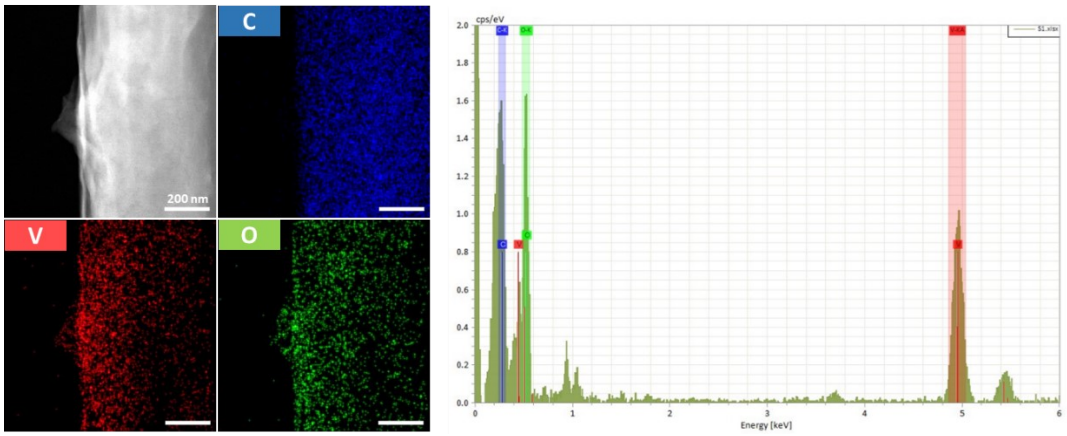

Figure S4. HAADF-STEM and EDS mapping images of VO_x/CNF electrodeposited for 10 min.

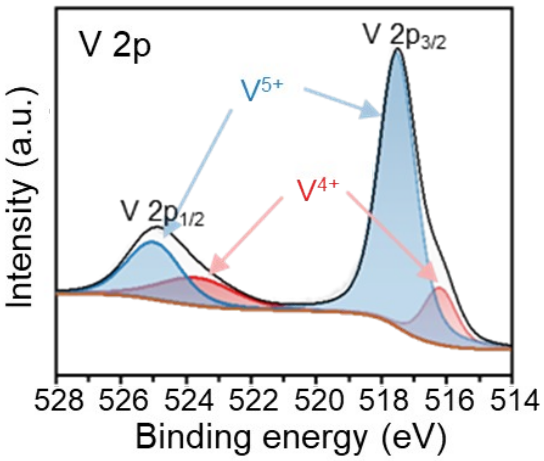

Figure S5. XPS V 2p spectra of VO_x/CNF before photothermal shock.

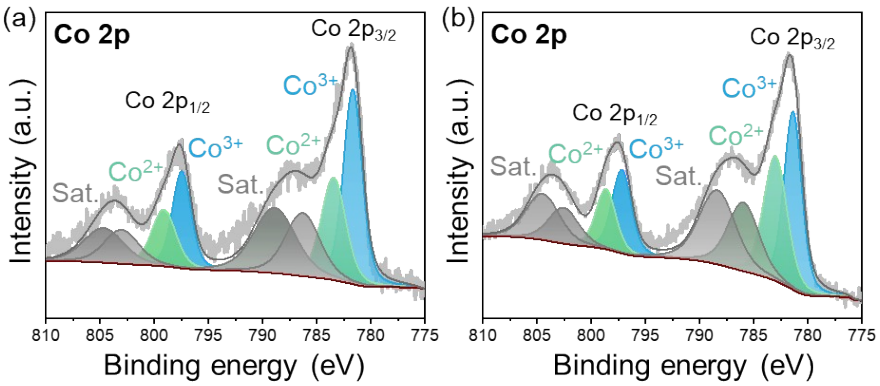

Figure S6. XPS Co 2p spectra of (a) Co/VOx/CNF-L and (b) Co/VOx/CNF-H.

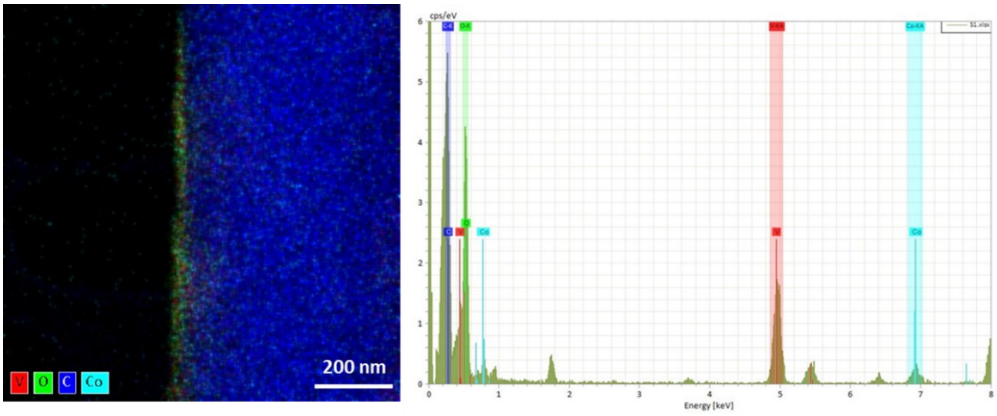

Figure S7. EDS mapping images of $Co/VO_x/CNF\text{-}H$.

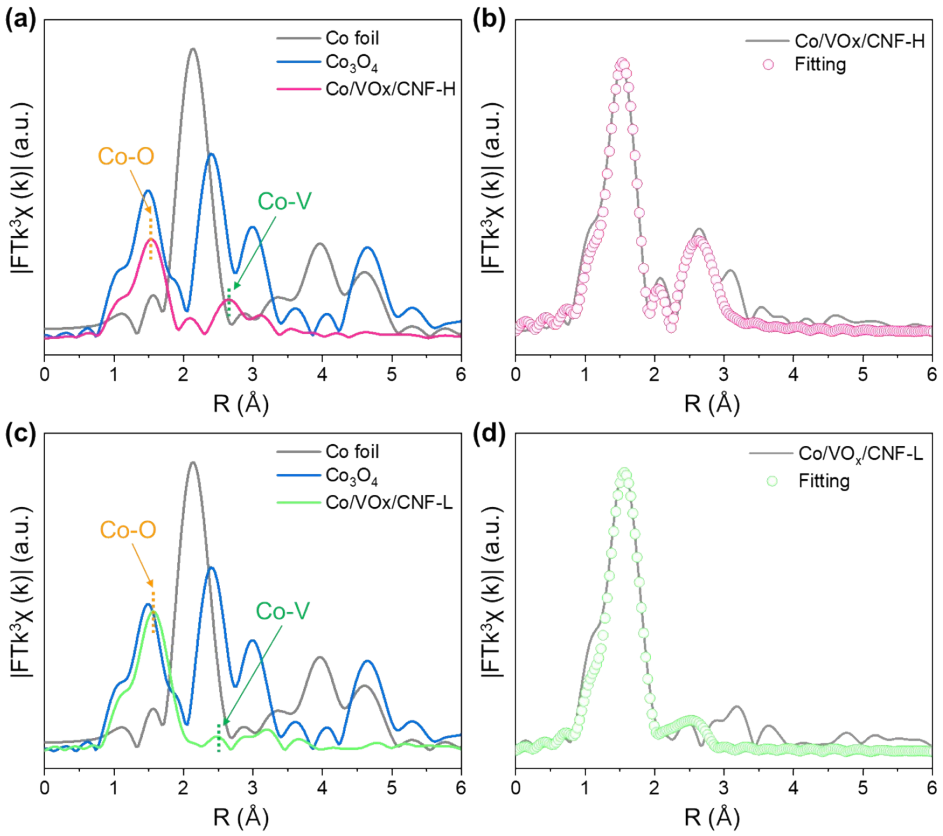

Figure S8. EXAFS data and fitting result of Co/VO_x/CNF-H and CO/VO_x/CNF-L.

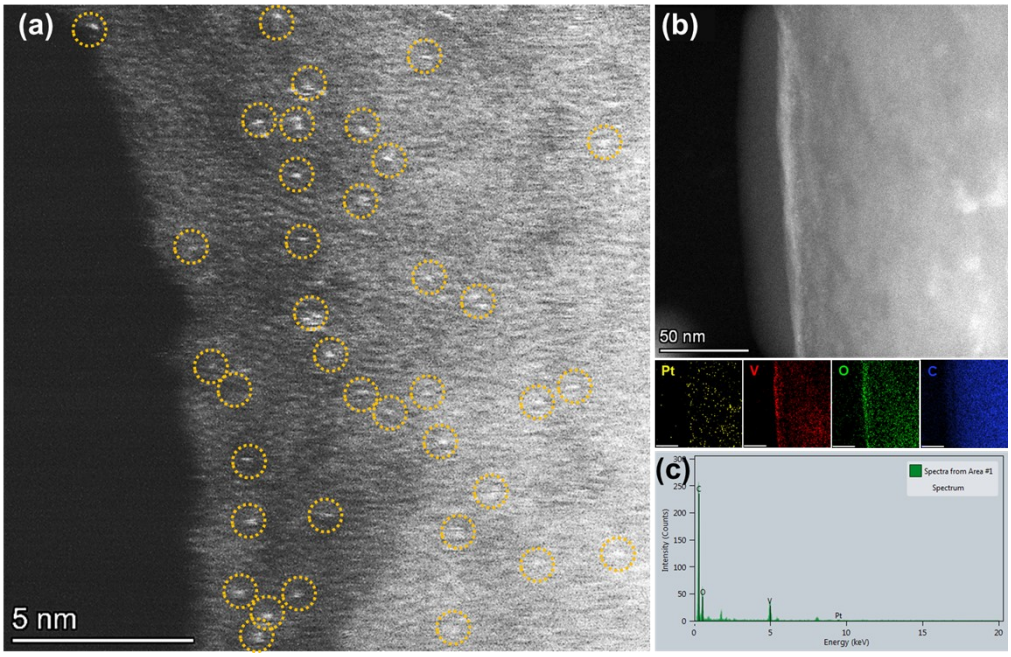

Figure S9. HAADF-STEM, EDS mapping images, and spectrum of Pt/VO_x/CNF.

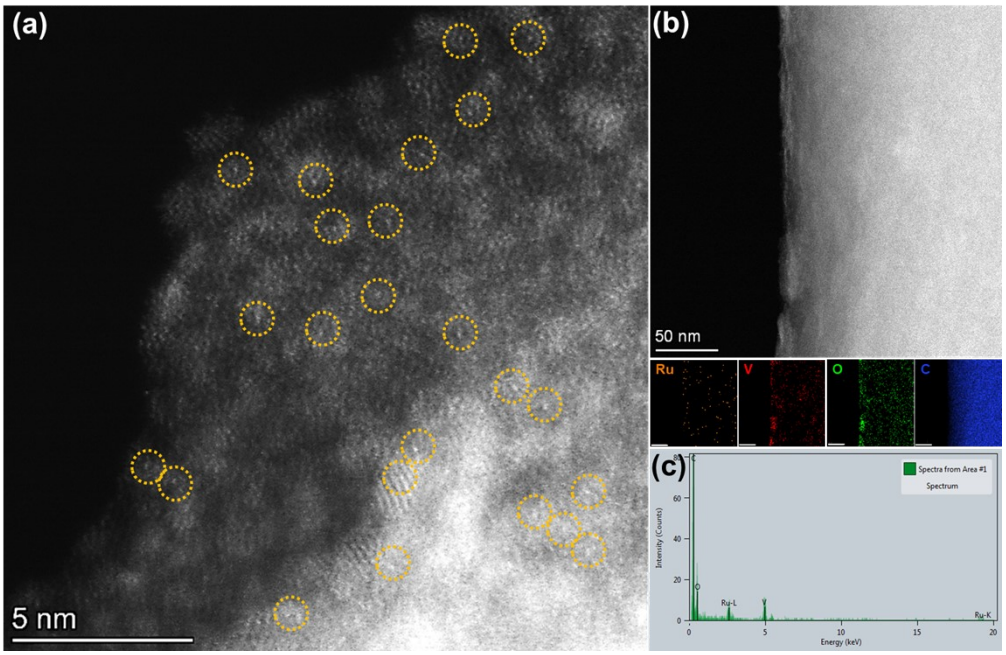

Figure S10. HAADF-STEM, EDS mapping images, and spectrum of Ru/VO_x/CNF.

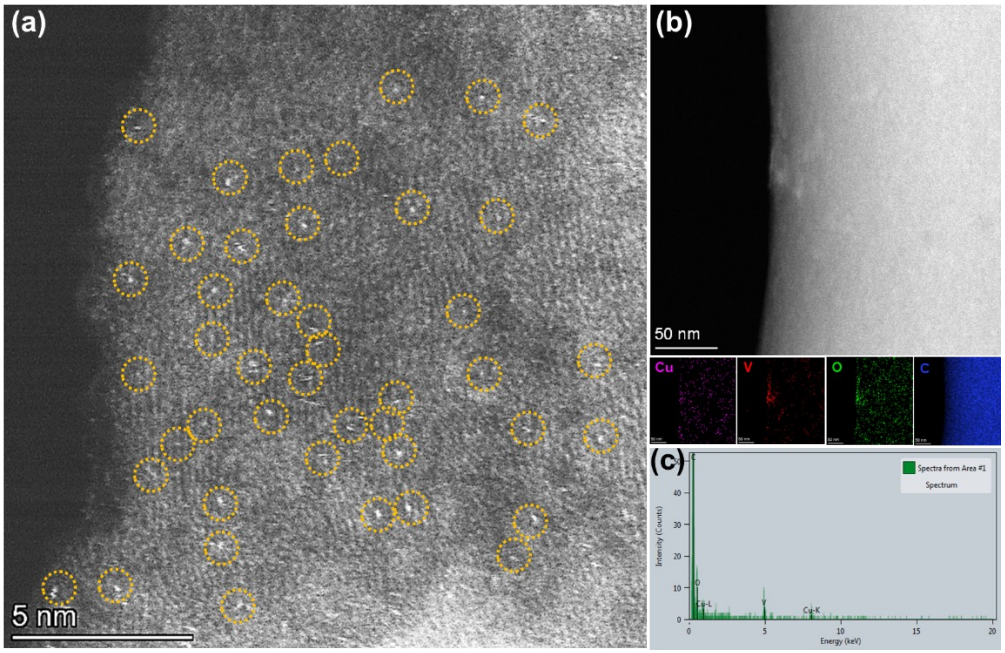

Figure S11. HAADF-STEM, EDS mapping images, and spectrum of Cu/VO_x/CNF.

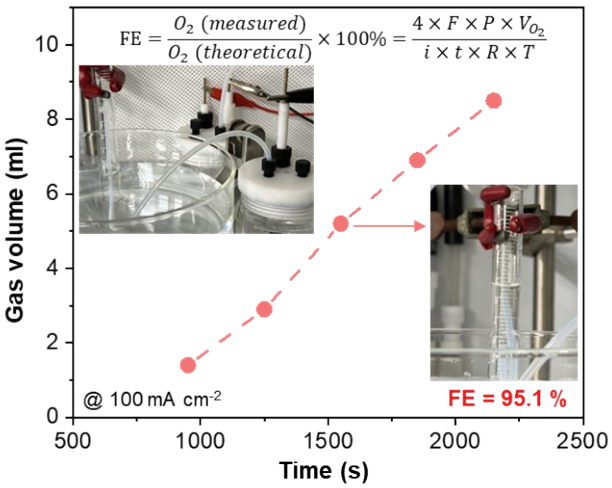

Figure S12. Quantitative analysis of Faraday efficiency.

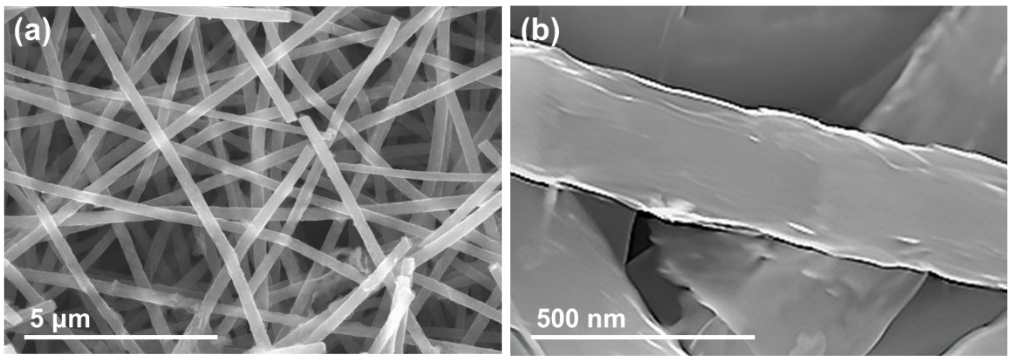

Figure S13. Post-OER structural characterization of Co/VO_x/CNF-H. Ex situ SEM images of Co/VO_x/CNF-H at (a) low and (b) high magnification after a 300-cycle durability test. The nanofibrous morphology remained intact, confirming the robust structural integrity of the catalyst under OER conditions.

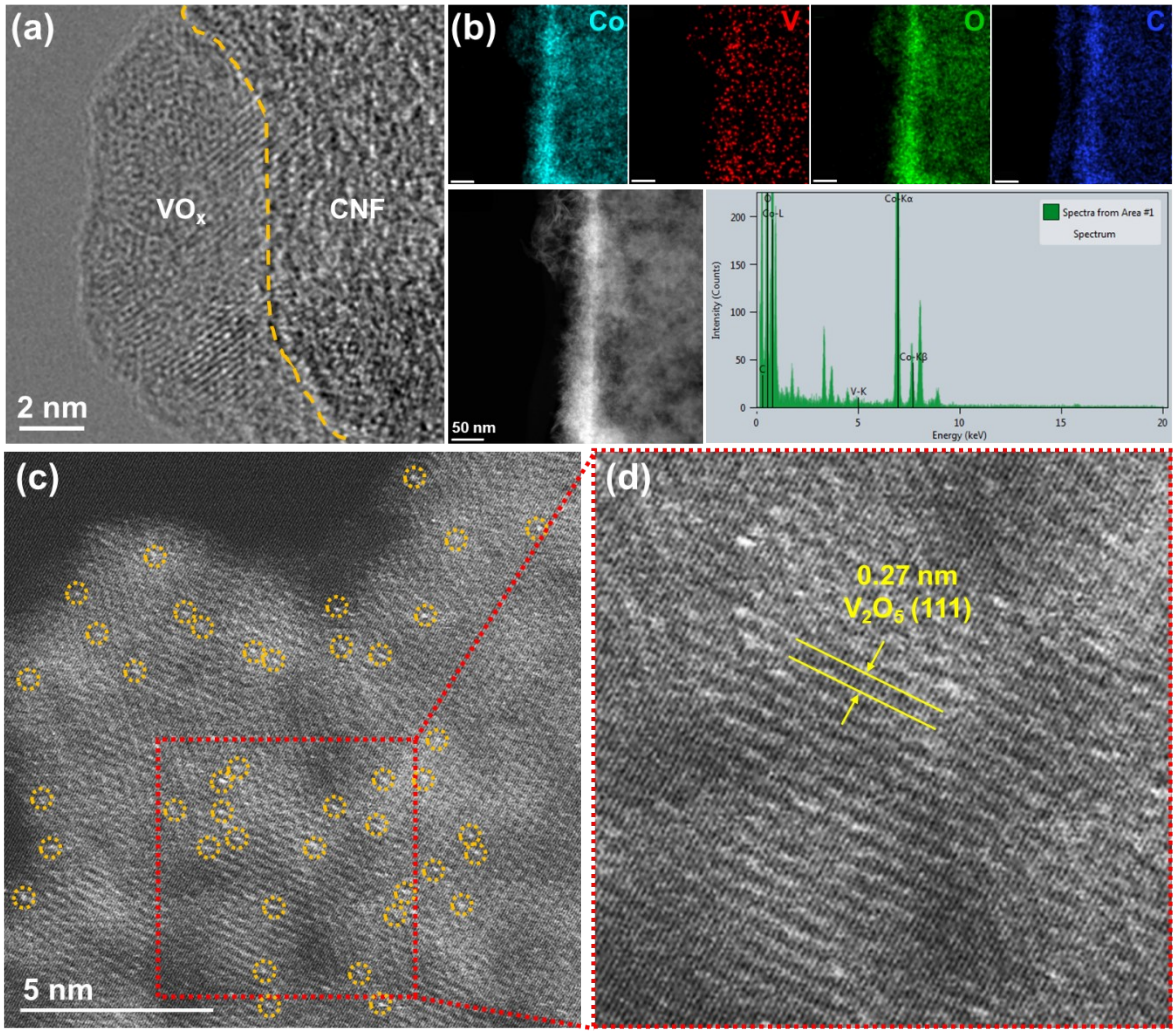

Figure S14. Post-OER electron microscopy and spectroscopy analyses of Co/VO_x/CNF-H. (a) TEM image highlighting of interfaces between VO_x and CNF, (b) EDS mapping image and spectrum, (c) HAADF-STEM images at (c) low and (d) high magnification after long-term stability test.

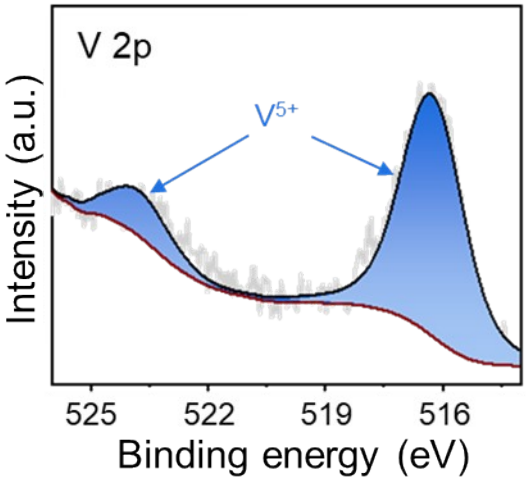

Figure S15. Ex situ XPS spectra of V 2p for Co/VO_x/CNF-H after the OER durability test.

Table S1. EXAFS fitting table of $Co/VO_x/CNF-H$ and $Co/VO_x/CNF-L$.

Sample	Shell	CN	R(Å)	σ^2	R factor
$Co/VO_x/CNF-H$	Co-O1	2.9	2.01	0.0041	0.0185
	Co-O2	1.9	2.18	0.0084	
	Co-V	0.7	3.00	0.0015	
$Co/VO_x/CNF-L$	Co-O1	2.9	2.01	0.0015	0.0179
	Co-O2	2.7	2.16	0.0022	
	Co-V	0.6	2.95	0.0084	

S_0^2= 0.72; CN: coordination number; R: bond length; distance between absorber and scatter atoms; σ^2: Debye-Waller factors; R-factor: goodness of fit.